Sensors & Actuators: B. Chemical 302 (2020) 127198

Contents lists available at ScienceDirect

Sensors and Actuators B: Chemical

journal homepage: www.elsevier.com/locate/snb

Fabrication of test strips with gold-silver nanospheres and metal–organic frameworks: A fluorimetric method for sensing trace cysteine in hela cells

Yuanyuan Cai, Yue Hua, Mengyuan Yin, Huan Liu, Shuai Li, Fengxiang Wang, Hua Wang*,[1]

Rizhao Key Laboratory of Marine Medicine and Materials Application Technologies, College of Chemistry and Chemical Engineering, Qufu Normal University, Qufu City, Shandong Province, 273165, PR China

ARTICLE INFO

Keywords:
Gold-silver nanospheres
Metal organic frameworks
Test strips
Fluorimetric analysis
Cysteine

ABSTRACT

A fluorimetric test strips-based strategy has been initially developed for probing trace cysteine (Cys) in hela cells using gold-silver (Au-Ag) nanospheres and metal-organic frameworks of ZIF-8. Bimetallic Au-Ag nanoclusters were first synthesized by the protein-templated biominerization and then harvested by a desolvation route to form Au-Ag nanospheres showing strong fluorescence that could be specifically quenched by Cys. The as-prepared nanospheres were coated onto test strips to be further shelled with ZIF-8 by using a vacuum-aided fast drying route with super-hydrophobic patterns. It was discovered that the so fabricated test strips could not only achieve uniform coatings of fluorescent nano-probes, but also the ZIF-8 shell-enabled improvement of fluorescence, environmental and storage stabilities. In addition to the evaluation of Cys in serum samples, the developed fluorimetric test strips can facilitate the direct detection of Cys in hela cells with the linear concentrations ranging from 0.0032 to 32.0 μM, thus promising for the point-of-care monitoring of low-level Cys for the clinical early diagnosis of some diseases like cancers. Besides, such a proposed protocol forthe fabrication of stable and uniform test strips using MOFs coatings and super-hydrophobic patterns may be tailored for designing various solid-state testing platforms for the extensive analysis applications.

1. Introduction

Cysteine (Cys) as a sulfur-containing amino acid plays a crucial role in human body with many biological functions in the metabolism and detoxification, especially the intramolecular crosslinking of proteins and reversible redox reactions inside cells [1–4]. The levels of Cys as amedical biomarker in body (i.e., blood and cells) can be highly associated with many diseases like hair depigmentation, edema, liver damage, skin lesions, and cancers [5–7], and capillary electrophoresis coupled with an optical or mass spectrometry detector [8–10]. Most of them, however, may suffer from some disadvantages like expensive instrumentation, time-consuming analysis procedure, and tedious pretreatment of samples, which may limit the scope of their practical applications especially for point-of-care monitoring. Therefore, exploring a fast, simple, and sensitive sensor for probing Cys is of great interest for the early diagnosis of various diseases.

Fluorimetric biosensors with some attractive analysis properties hold a great promise for delivering a fast and sensitive detection diagnosis in various biomedical settings [8–18]. However, most of fluorimetric analysis technologies with bulky fluorescent spectrophotometer including those for probing Cys [19,20], may not be suitable for the direct and point-of-care evaluation of analytes. Alternatively, some efforts have been devoted to the fabrication of solid phase-based fluorimetric sensors like the ones using test strips [21–24]. Moreover, it is well established that the analysis performances of fluorimetric biosensors can largely depend on the optical and physiochemical properties of fluorescent probes such as the FL intensities and environmental stability [25]. In recent years, noble metal nanomaterials, most known as Au and Ag nanoclusters, have received increasing attentions in serving as the preferable candidates of fluorescent probes, due to their some outstanding merits like high fluorescence (FL) intensities for the fluorimetric detections [26–31]. For example, Yu et al reported the preparation of Au nanoclusters with tunable optical properties separately for sensing Cu^{2+} ions and Ag^{+} ions [32]. Xie's group synthesized Ag nanoclusters for the sensitive detection of Cys [19]. Our group also prepared bimetallic Au nanoclusters with silver-enhanced FL for the simultaneous detections of Cu^{2+} and Hg^{2+} ions [33]. In particular, Au or Ag nanomaterials have been utilized increasingly for the design of fluorimetric test strips [22,34]. Yet, a formidable challenge regarding the storage and environmental stability

* Corresponding author.
E-mail address: huawang@qfnu.edu.cn (H. Wang).
[1] http://wang.qfnu.edu.cn.

https://doi.org/10.1016/j.snb.2019.127198
Received 27 March 2019; Received in revised form 23 August 2019; Accepted 25 September 2019
Available online 27 September 2019
0925-4005/

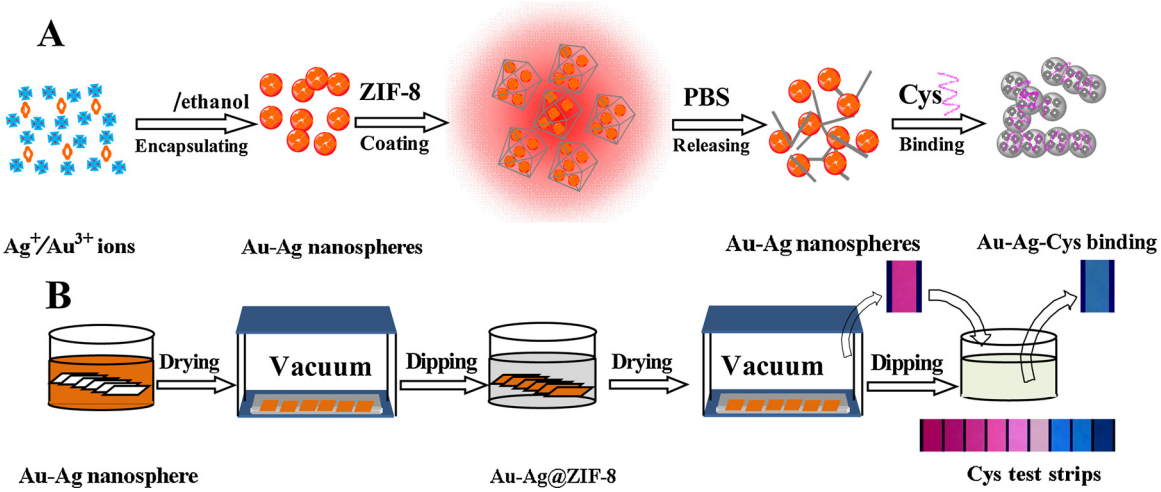

Scheme 1. (A) Schematic illustration of the main procedure and mechanism of fluorimetric Au-Ag@ZIF-8-based test strips for probing Cys, including Au-Ag coating, ZIF-8 shelling, and Cys tests by dipping, in which the hydrophobic pattern-aided drying preparation of strips were performed in vacuum. (B) The main reactions for sensing Cys, including the BSA encapsulation-based preparation of Au-Ag nanospheres, and the ZIF-8 shelling and PBS-triggered release of Au-Ag@ZIF-8, followed by the Cys-induced fluorescence quenching of Au-Ag@ZIF-8.

(i.e., optical blenching) may be encountered for the fluorescent probes like photosensitive Ag nanomaterials especially coated on test strips, which might prohibit the fluorimetric test strips from the large-scale analysis applications.

In the present work, we seek to fabricate fluorimetric test strips for probing trace-level Cys in hela cells and serum samples by using protein-encapsulated bimetallic gold-silver (Au-Ag) nanospheres. These gold-silver (Au-Ag) nanospheres were initially synthesized to combine with metal-organic frameworks (MOFs) of ZIF-8 acting as the robust fluorescent nano-probes, with the main fabrication procedure shown in Scheme 1. Herein, bovine albumin serum (BSA) was employed as the protein template to fabricate the bimetallic Au-Ag nanoclusters through the biominerization route. The resulting products were further harvested by the desolvation method using ethanol to replace water, thus forming Au-Ag nanospheres. It was discovered that the obtained Au-Ag nanospheres could present considerably high FL intensities that could be specifically quenched by Cys. Moreover, the fluorescent nanospheres were coated onto test strips for sensing Cys, in which a vacuum-aided fast drying route with super-hydrophobic patterns were introduced designedly to suppress the “Coffee stains” toward the uniform strips. Nevertheless, the so fabricated test strips were experimentally explored to display still low environmental and storage stabilities over time. Alternatively, ZIF-8 MOFs were utilized to shell the Au-Ag-coated test strips, achieving greatly improved photo-stability and storage stability. What’s more, further enhanced FL intensities of test strips could be expected. Subsequently, the as-prepared fluorimetric test strips were demonstrated in the evaluation of Cys in hela cells and serum samples, showing high analysis selectivity, sensitivity, and reproducibility. To the best our knowledge, this is the first success on the design of fluorimetric test strips coated with Au-Ag nanospheres and MOFs for sensing Cys in biological samples like hela cells.

2. Experimental section

2.1. Reagents

Tetrachloroauric acid ($HAuCl_4$, 99.9%), silver nitrate ($AgNO_3$), bovine serum albumin (BSA), cysteine (Cys), alanine (Ala), serine (Ser), leucine (Leu), glycine (Gly), lysine (Lys), phenylalanine (Phe), histidine (His), tryptophan (Trp), trytophan (Try), glutamate (Glu), valine (Val), arginine (Arg), threonine (Thr), asparagines (Asn), isoleucine (Ile), proline (Pro), and aspartic acid (Asp), dopamine (DA), and glutathione (GSH) were purchased from Sigma-Aldrich (Beijing, China). Zinc acetate, 2-methylimidazole, and phosphate buffered saline (PBS) were purchased from Beijing Chemical Reagent Co. (Beijing, China). Hexadecyltrimethoxysilane (HDS), and ethanol were purchased from Sinopharm Chemical Reagent Co., Ltd (Shanghai, China). HeLa cells were purchased from Shanghai SunBio Biomedical technology Co., Ltd. All of the other chemicals are of analytical grade, and all glass containers were cleaned by aqua regia and ultrapure water before usage. Whatman filter papers used for water test strips were purchased from Sigma-Aldrich (Beijing, China). Deionized water (18 MΩ) was supplied from an Ultra-pure water system (Pall, USA).

2.2. Apparatus

The fluorescence (FL) measurements were conducted using Fluorescence spectrophotometer (Horiba, FluoroMax-4, Japan) operated at an excitation wavelength at 470 nm, with both excitation and emission slit widths of 5.0 nm. Transmission electron microscopy (TEM, JEM-2100PLUS, Japan) imaging operated at 100 kv was employed to separately characterize the morphological structures of Au-Ag and Au-Ag@ZIF-8 nano-probes. The Cys Assay Kits was purchased from Sigma-Aldrich (Beijing, China). The Table centrifuge (Thermo Scientific, Deutschland) was used in the preparation and purification procedures.

2.3. Synthesis of Au-Ag nanospheres

BSA powder was dissolved in water with a concentration of 40 mg/mL and pH 9.0 adjusted. The BSA solution was first stirred for 2.0 h at room temperature and then overnight (8 h) at 4 °C to complete the hydration of protein molecules. An aliquot of $HAuCl_4$ (2.0 mL, 10 mM) was added to the above treated BSA (2.0 mL, 40 mg/mL). Then, $AgNO_3$ (0.80 mL, 8.0 mM) was added under vigorous stirring for 5.0 min at 37 °C. Afterwards, NaOH solution (0.20 mL, 1.0 M) was introduced in the mixture to be incubated at 37 °C for 12 h. Further, the resulting solution was dialyzed in water for 48 h. Moreover, the resulting BSA-encapsulated Au-Ag nanoclusters were desolvated with ethanol according to a modified route previously reported [35]. Typically, ethanol was introduced by drop wise at the BSA-to-ethanol volume ratio of 1/4 under the constant stirring at 1200 rpm by using a syringe pump with a flow rate of 1.0 mL per minute. After the desolvation, the suspensions were diluted in water (1/100) so as to reduce the concentration of desolvating agent below 1.0%. The so yielded Au-Ag nanospheres were stored in dark at 4 °C.

2.4. Preparation of fluorimetric Cys test strips

The Cys test strips were fabricated by being coated first with Au-Ag nanospheres and then ZIF-8 according to a modified preparation route reported previously [22]. Herein, the test strips were fabricated by using the super-hydrophobic patterns to work with the fast drying in vacuum, which would aid to depress the formidable "coffee strains" to achieve the uniform coatings of fluorescent nano-probes on test strips. Herein, the super-hydrophobic patterns were fabricated by coating HDS onto the glass substrates (72 × 24 mm^2) that were firstly cleaned with the piranha solution (H_2SO_4 : H_2O_2 = 7 : 3), and then thoroughly washed and dried in nitrogen. Furthermore, the cleaned substrates were dipped into the HDS solutions in ethanol to be reacted for 6.0 h at room temperature. The so prepared super-hydrophobic HDS patterns were kept in the sealing drier for future usage. Moreover, glass filter papers were cut into the slices of test strips (10 mm × 10 mm), and then immersed into the Au-Ag suspension (0.20 mg/mL) for 10 min. After that, the resulting strips were immediately placed onto the super-hydrophobic HDS patterns above to be dried in vacuum for 20 min. Furthermore, the strips were dipped into the mixture containing zinc acetate dihydrate (40 mM, 2.0 mL) and 2-methylimidazole (160 mM, 2.0 mL) for 8 min. After that, these strips were immediately placed onto the super-hydrophobic HDS patterns again to be dried in vacuum for 20 min. The so obtained Cys test strips were stored in dark for future use.

2.5. Fluorimetric test strips-based analysis for Cys

The detection conditions of the fluorimetric test strips-based assays were firstly optimized, mainly including pH values (1.0, 3.0, 5.0, 7.0, 9.0, 11.0, and 13.0), temperature (4.0, 20.0, 37.0, 50.0, 70.0, and 90.0 °C), ionic strengths (0, 100, 200, 300, 400, and 500 mM NaCl) and reproducibility (seven times). Under the optimized conditions, the fluorimetric Au-Ag@ZIF-8-based test strips were applied for probing Cys with different concentrations in buffer (0.0010, 0.0050, 0.010, 0.050, 0.10, 0.50, 1.0, 5.0, and 10.0 μM). The Cys-induced FL quenching efficiencies of test strips were recorded by the FL spectrometer with a holder for the solid-state FL measurements. In addition, the control tests were separately conducted accordingly for different analytes (1.0 μM) of amino acids (Cys, Ala, Ser, Leu, Gly, Lys, Phe, His, Trp, Tyr, Glu, Val, Arg, Thr, Asn, Ile, Pro, and Asp), DA, GSH,Cu^{2+}, Na^+, Mg^{2+}, Ca^{2+}, Zn^{2+}, Fe^{2+}, and Fe^{3+}ions. Herein, the quenching efficiencies were calculated according to the following equation: quenching efficiencies = $(F_0\text{-}F)/F_0 \times 100\%$, where F_0 and F refer to the FL intensities of the Au-Ag@ZIF-8-based test strips in the absence and presence of Cys, respectively.

2.6. Preliminary application of test strips for probing Cys in samples

The extraction of intracellular Cys from Hela cells was first performed according to the reported procedure [36]. Typically, hela cells lines were incubated in DMEM containing glucose and fetal bovine serum (10.0%) in a humidified incubator (5.0% CO_2 - 95.0% air) at 37 °C. After being harvested through trypsinization, the cells were centrifuged (3000 rpm, 5 min), washed, and then re-dispersed in PBS solution. Furthermore, the cell lysates were obtained using Radio immunoprecipitation assay lysis buffer (100 μL) to be further centrifuged (12,000 rpm, 20 min). The intracellular Cys concentrations in the resulting samples of supernatants were determined according to the colorimetric instruction available in the Cys Assay Kit. Subsequently, the Au-Ag@ZIF-8-based test strips were applied for the fluorimetric evaluation of Cys of different concentrations spiked in hela cells extractions (0.00032, 0.0020, 0.032, 0.10, 0.32, 1.0, 3.20, 10, and 32.0 μM), of which the Cys-induced FL quenching efficiencies were recorded by the FL spectrometer with a holder for the solid-state FL measurements. Besides, the fluorimetric test strips were accordingly employed to evaluate Cys with different concentrations spiked in human serum. All the experiments of sample analysis were performed in compliance with the Ethical Committee Approval of China, and approved by the ethics committee at Qufu Normal University.

3. Results and discussion

3.1. Main procedure and mechanism for the Au-Ag@ZIF-8-based fluorimetric Cys analysis

It is well established that the protein-templated biominerization way is a highly efficient method for the controllable synthesis of some noble metals nanomaterials like Au or Ag nanoclusters [19,37,38], as well as the formation of MOFs like ZIF-8 [30,31]. In the present work, Au-Ag@ZIF-8 nano-probes were fabricated accordingly for sensing Cys, with the main procedure and mechanism schematically illustrated in Scheme 1A. Herein, bimetallic alloying Au-Ag nanoclusters were first synthesized using BSA and Au/Ag precursors through the biomineralization process. The resulting Au-Ag nanoclusters were further harvested according to a desolvation route by using ethanol to replace water [35], so as to yield the BSA-encapsulated Au-Ag nanospheres. Further, the obtained nanospheres were encapsulated into ZIF-8 matrix to yield the Au-Ag@ZIF-8, displaying greatly enhanced FL intensities. More importantly, the ZIF-8 shells could be collapsed once dispersed in phosphate-containing buffer like PBS because of the stronger Zn^{2+}-phosphate interactions, of which the released Au-Ag cores would specifically bind with Cys resulting in the FL quenching. Moreover, the as-fabricated Au-Ag nanospheres were alternatively coated onto filter papers to be further shelled with ZIF-8 to produce the fluorimetric test strips for probing Cys. The fabrication and sensing procedures are schematically described in Scheme 1B. Notably, a vacuum-aided fast drying route was designedly introduced with super-hydrophobic patterns to suppress the "Coffee stains" through a fabrication route proposed previously in our group [22], so as to achieve the uniform products of test strips. The developed Au-Ag@ZIF-8-based fluorimetric test strips were applied practically for the real-time evaluation of trace Cys separately in hela cells and serum samples afterwards.

3.2. Cys-response performances of the fluorimetric test strips

A comparison of Cys responses was performed between the fluorimetric test strips coated with fluorescent nano-probes ofAu-Ag@ZIF-8 and Au-Ag (Fig. 1A). It was discovered that the Au-Ag@ZIF-8 test strip could present the enhanced FL intensity (curve a), which is about 1.5-time brighter than that of the Au-Ag one (curve c). More importantly, the Cys-induced FL quenching of the Au-Ag@ZIF-8 test strip (curve b) is more than 2.0-time larger than that of the Au-Ag one (curve d). Such a fact can also be visualized comparably for the Au-Ag-coated test strips with and without ZIF-8 shells (Fig. 1A, insert). Herein, the ZIF-8 shells with nitrogen-containing organic ligands like imidazole groups might conduct the well-known "electron donor effects" towards the increased FL intensities of Au-Ag cores in Au-Ag@ZIF-8, as observed elsewhere for the amine-containing ligands [39]. Particularly, the ZIF-8 matrix might modulate Au-Ag cores within the rigid framework of MOFs so as to spatially separate them in certain orientations in Au-Ag@ZIF-8, thus showing further improved luminescence and enhanced aqueous stability [40]. Especially, the strong Ag-Cys interaction should specifically trigger the FL quenching of the test strips as described elsewhere for the Cys-induced FL quenching of Ag nanoclusters [19]. More importantly, the Au-Ag@ZIF-8 test strips could show much higher FL response to Cys, indicating the vital role that the ZIF-8 shells might play in sensing Cys especially on test strips.

Furthermore, a comparison of UV–vis spectra was conducted between Au-Ag@ZIF-8 and Au-Ag nano-probes in PBS in the presence and absence of Cys (Fig. 1B). One can note that Au-Ag@ZIF-8 can be suspended well in PBS, which however could become even clear after

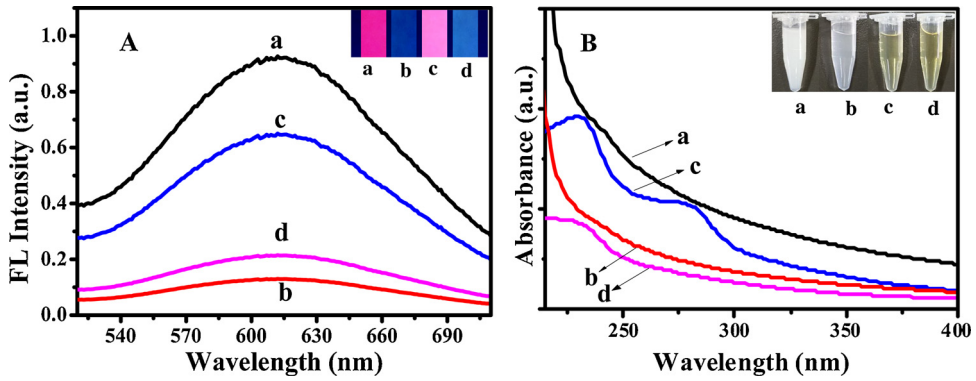

Fig. 1. (A) Normalized FL spectra of test strips and (B) UV–vis spectra of (a) Au-Ag@ZIF-8 and (c) Au-Ag, and (b, d) the ones after adding Cys, respectively (insert: the photographs of corresponding product solutions under UV or white light).

adding Cys, as visually shown in the photographs (Fig. 1B, insert). It implies that ZIF-8 shells of Au-Ag@ZIF-8 probes might be collapsed in the phosphate-containing PBS because of stronger Zn^{2+}-phosphate interaction to produce zinc phosphate, whereas the released Au-Ag cores would conduct the binding with Cys. Yet, they might display no obvious absorption peak in PBS both in the absence (curve a) and presence (curve b) of Cys, except for the adsorption that might be reduced to some degree after adding Cys. In contrast, Au-Ag probes could present an absorption peak at 275 nm (curve c), which might disappear after adding Cys (curve d). The data indicate that the developed Au-Ag@ZIF-8 nano-probes could response to Cys, in which the introduction of ZIF-8 shells could further improve their performances in sensing Cys.

3.3. Fabrication and characterization of nano-probes for sensing Cys

The main fabrication conditions were optimized for the Au-Ag@ZIF-8 nano-probes, in which the Au-Ag nanospheres were fabricated to be further shelled with ZIF-8 (Fig. 2). As described in Fig. 2, the largest quenching efficiency induced by Cys at the same concentration was obtained at the Au-to-Ag molar ratio of 25/8,although it might not present the largest FL intensity (Fig. 2A, insert).The data indicate that there should be a most suitable Au-Ag proportion in the fluorescent probes (i.e., 25/8) available for specifically binding with Cys towards the FL quenching, as confirmed previously for these with the strongest "silver effect"-enhanced red fluorescence [33]. Moreover, Fig. 2**B** discloses the effects of the mass ratios of Au-Ag to ZIF-8 on the Cys-induced quenching efficiencies. Obviously, the greatest FL quenching efficiency of probing Cys was achieved at the mass ratio of Au-Ag to ZIF-8 of 1/2, together with the maximum FL intensity (Fig. 2B, insert).

The topological changing structures of fluorescentAu-Ag@ZIF-8 and Au-Ag nano-probes in probing Cys were comparably characterized by transmission electronic microscopy (TEM) imaging (Fig. 3). As can be seen from Fig. 3A, Au-Ag nano-probes could be fabricated with well-defined nanospheric structure with the size of about 100 nm in diameter, consisting of numerous alloying Au-Ag nanoclusters, as revealed apparently in the amplified image (insert). Once Au-Ag nanospheres were encapsulated into the ZIF-8 matrix, the so yielded Au-Ag@ZIF-8 could exhibit the defined cubic structure of ZIF-8 MOF profile with a length of about 1.0 μm (Fig. 3B), as clearly shown in the amplified view (insert). More interestingly, when Au-Ag@ZIF-8 nano-probes were dispersed in the phosphate-containing PBS, the ZIF-8 shells could be collapsed to release Au-Ag cores (Au-Ag nanospheres) because of the formation of zinc phosphate as aforementioned (Fig. 3C). Moreover, Fig. 3E manifests a high-resolution image of the released Au-Ag cores, showing that they were filled with Au-Ag nanoclusters with a size of about 5.0 nm in diameter. Furthermore, after Cys was added, most of these Au-Ag cores could be cross-linked and then aggregated (Fig. 3D). In particular, Cys would also enter and interact with the BSA-encapsulated Au-Ag nanoclusters resulting in the structure decomposition as disclosed in the high-resolution image (Fig. 3F). Importantly, the Cys-induced structure change of Au-Ag cores could trigger the FL quenching of Au-Ag@ZIF-8 as demonstrated in Fig. 1**A** above. Such a phenomenon might be attributed to two reasons. On the one hand, the introduction of zwitterionic Cys with isoelectric point of 5.02 might bind with BSA-encapsulated Au-Ag cores (nanospheres), which were released from the Au-Ag@ZIF-8 dispersed in PBS, so that the preferential self-assembly of nanospheres would occur in an end-to-end fashion through a two-point electrostatic interaction towards the agglomeration of nanospheres leading to the FL quenching (Fig. 3D), as described elsewhere for the Cys-bound Au nanorods [41]. On the other hand, Cys with thiol groups would enter the Au-Ag cores to etch Ag atoms on their surfaces due to the strong Ag-S interactions [19]. As a result, the structure decomposition of Au-Ag nanoclusters might take place yielding the smaller ones or even the nonluminous thiolate-Ag (I) complexes (Fig. 3F). Yet, the detailed mechanism should be further explored in the future work.

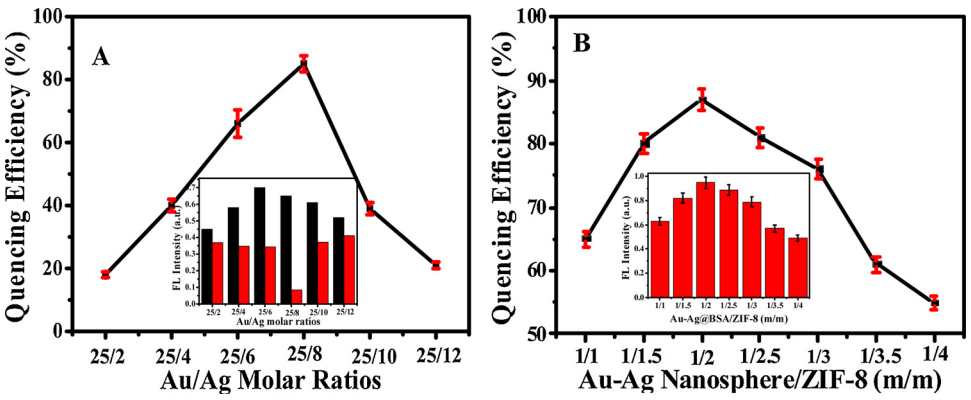

Fig. 2. Optimization of main fabrication conditions forAu-Ag@ZIF-8 with the Cys(1.0 μM)-induced FL quenching efficiencies separately depending on (A) the Au-to-Ag molar ratios (insert: FL intensities of the ones in the absence (black) and presence (red) of Cys) and (B) the mass ratios of Au-Ag to ZIF-8 (insert: the FL intensities). (For interpretation of the references to colour in this figure legend, the reader is referred to the web version of this article).

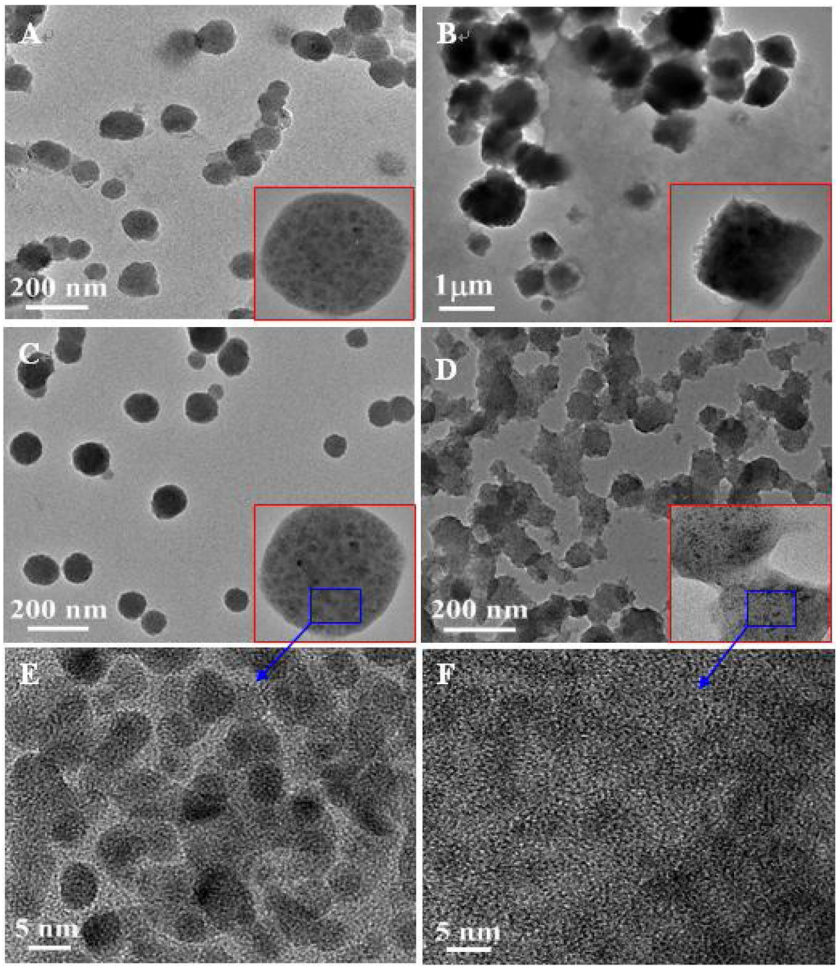

Fig. 3. TEM images of (A) Au-Ag, (B) Au-Ag@ZIF-8, and (C) Au-Ag@ZIF-8 in PBS followed by (D) adding Cys (insert: the amplified particles), showing (E, F) the corresponding Au-Ag nanoclusters encapsulated, respectively.

3.4. Environmental stability of Au-Ag@ZIF-8-coated test strips

The fluorimetric Cys test strips were fabricated by being coated first with Au-Ag nanospheres and then ZIF-8 MOFs aforementioned. The environmental stability of the so prepared fluorimetric test strips were investigated in sensing Cys under the harsh conditions, in comparison with the ones without ZIF-8 shells (Fig. 4). Fig. 4A manifests a comparison of storage stability between the Au-Ag-coated test strips with and without ZIF-8 shells. It was found that the ZIF-8 shells could endow the test strips with basically maintained FL intensities, even stored for eight months (black), whereas the ones without ZIF-8 shells could display some decays in the FL intensities (red). Fig. 4B exhibits the comparable results of optical stability among the Au-Ag-coated test strips with and without ZIF-8 shells, which were separately exposed to the xenon lamp over different time intervals. One can note that the ZIF-8-shelled test strips could display no significant change of FL intensities even exposed to the strong light up to 5.0 h (black), in contrast to the ones without ZIF-8 shells showing a dramatically decreased FL intensities (red). Accordingly, the introduction of ZIF-8 shells to the test strips with improved environmental stability against possible light bleaching and self-quenching in storage. Besides, further improved FL intensities could also be attained for the developed Cys test strips as validated in Fig. 1A above.

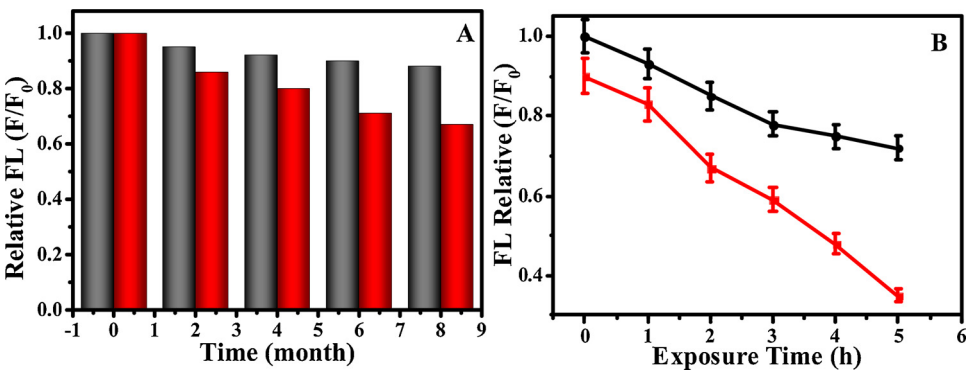

Fig. 4. Comparison of (A) storage and (B) light exposure stabilities between the Au-Ag-coated test strips with (black) and without (red) ZIF-8 shells, with the changing relative FL intensities depending on the time intervals of storage in dark at 4 °C and exposure under xenon lamp, respectively. (For interpretation of the references to colour in this figure legend, the reader is referred to the web version of this article).

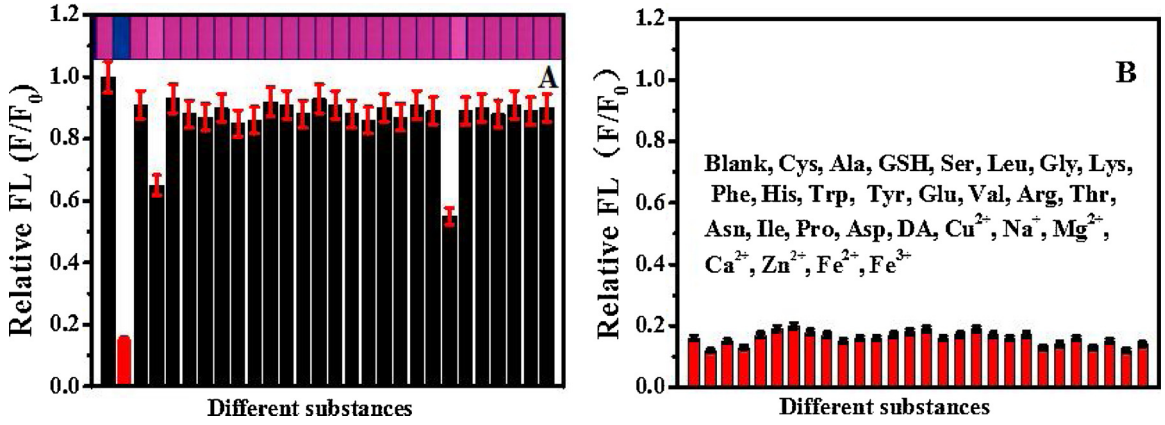

Fig. 5. Fluorimetric responses of Au-Ag@ZIF-8-based test strips to (A) different substances alone (1.0 μM) in order including blank, Cys, Ala, GSH, Ser, Leu, Gly, Lys, Phe, His, Trp, Tyr, Glu, Val, Arg, Thr, Asn, Ile, Pro, Asp, DA, Cu^{2+}, Na^{+}, Mg^{2+}, Ca^{2+}, Zn^{2+}, Fe^{2+}, and Fe^{3+} ions; and (B) Cys separately in the presence of one of these analytes (insert: corresponding photographs of testing solutions under UV light).

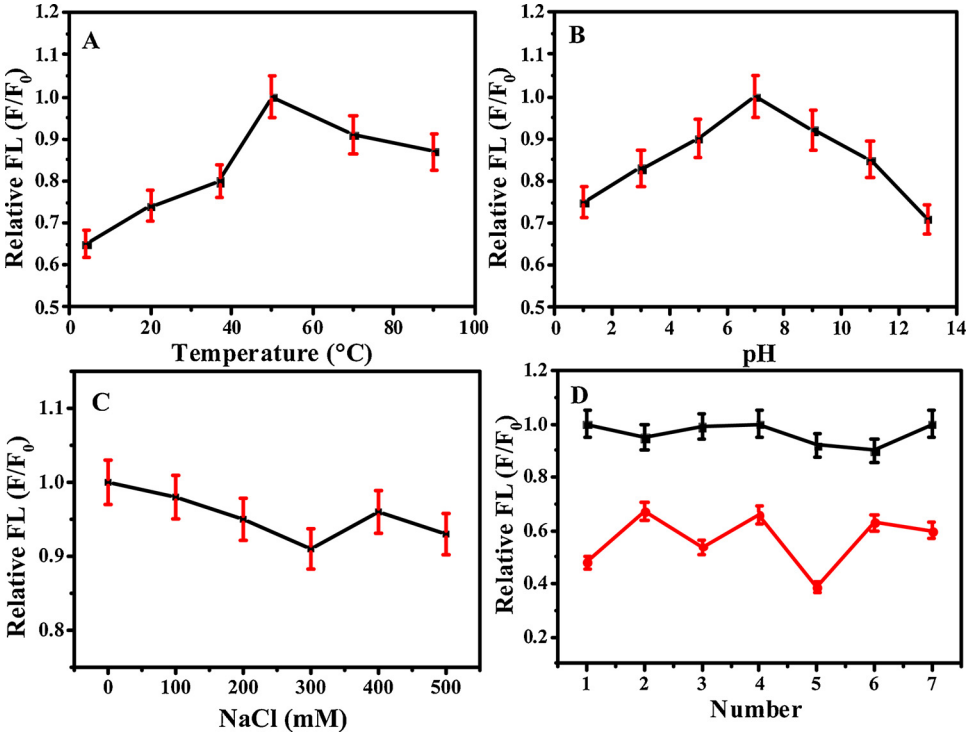

Fig. 6. Fluorimetric Cys detections of Au-Ag@ZIF-8-based test strips with relative FL intensities depending on (A) temperature, (B) pH values, (C) ion strengths in NaCl concentrations, and (D) comparison of analysis reproducibility between the test strips based on Au-Ag@ZIF-8 (black) and Au-Ag (red). (For interpretation of the references to colour in this figure legend, the reader is referred to the web version of this article).

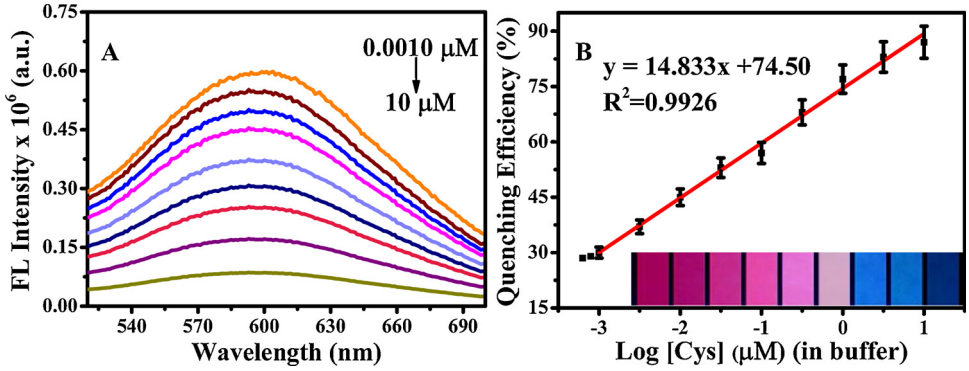

Fig. 7. (A) Normalized FL spectra of Au-Ag@ZIF-8-coated test strips with responses to Cys of different concentrations in buffer; (B)the calibration curve of FL quenching efficiencies versus the logarithmic concentrations of Cys in buffer (insert: photographs of corresponding testing solutions on the Au-Ag@ZIF-8-based test strips under UV light).

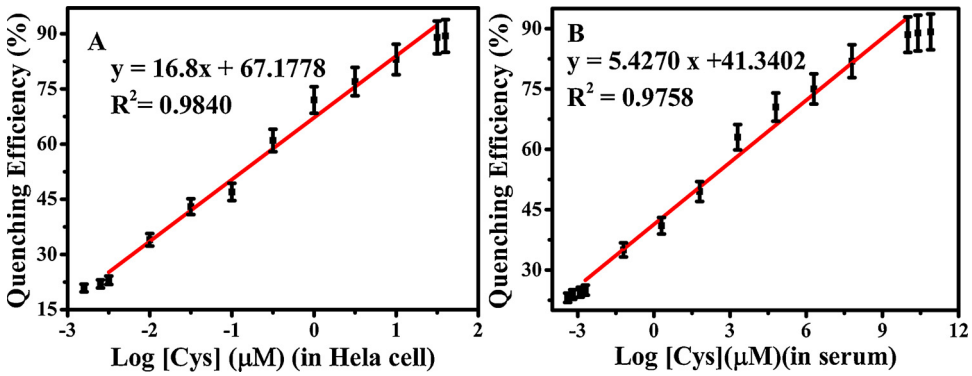

Fig. 8. The calibration curves of FL quenching efficiencies versus the logarithmic concentrations of Cys spiked separately in (A) cells extractions and (B) human serum samples.

3.5. Selective tests of fluorimetric Cys test strips

The fluorimetric sensing selectivity of the developed Cys test strips with Au-Ag@ZIF-8 coatings was systematically explored for probing Cys in comparison with some possibly co-existing substances including amino acids, GSH, dopamine (DA), and some metal ions like Cu^{2+} ions (Fig. 5). It was found from Fig. 5A that the tested amino acids exhibited no FL change of test strips, as apparently shown in corresponding photographs (Fig. 5A, insert). Yet, GSH and Cu^{2+} ions could trigger the FL quenching of the test strips to some degree, of which the quenching efficiencies, however, were much smaller than that of Cys. Of note, it is established that the concentrations of GSH in hela cells are commonly at the fmol-scale [42], which is too low to conduct any effect on the practical detection of Cys with much higher μM- level in hela cells [43]. Also, the possible effect of Cu^{2+} ions on the Cys detection could be circumvented by adding the Cu^{2+} chelating reagent of EDTA. More importantly, the fluorescent responses of test strips to Cys separately coexisting with the other analytes were investigated, showing no significant interference on the Cys analysis (Fig. 5B). The data indicate that the developed fluorimetric test strips could serve as the robust testing platform for the selective detection of Cys in some complicated biological media like cell extractions and blood.

3.6. Main analysis conditions of fluorimetric Cys test strips

The main detection conditions of the developed Au-Ag@ZIF-8test strips for probing Cys were optimized (Fig. 6). The fluorimetric responses to Cys were firstly studied under different pH conditions, showing the optimal pH value at 7.0 (Fig. 6A). Also, the optimal temperature for sensing Cys was determined to be at 37 °C (Fig. 6B). Moreover, one can note from Fig. 6C that there is no significant effect of ion strengths on the responses to Cys, which could be tested in the buffer with NaCl concentrations up to 500 mM. In addition, the detection reproducibility of Au-Ag@ZIF-8-coated test strips for Cys was examined by comparing to the ones without ZIF-8 shells (Fig. 6D). It was discovered that no obvious fluctuations of Cys responses was witnessed for the test strips during the repeated tests of seven times, in contrast to the ones without ZIF-8 shells. Therefore, the developed fluorimetric test strips can possess improved reproducibility in sensing Cys due to the shelling of ZIF-8 MOFs.

3.7. Fluorimetric test strips-based analysis for Cys in samples

Under the optimized conditions, the developed fluorimetric test strips were employed for detecting Cys of different concentrations spiked in buffer (Fig. 7). As shown in Fig. 7A, increasing Cys concentrations could induce the rationally decreases in the FL intensities of the test strips. Fig. 7B shows a calibration curve of FL quenching efficiencies versus the logarithms of Cys concentrations linearly ranging from 0.0010 to10.0 μM (R^2 = 0.9926), with the limit of detection of about 0.50 nM, estimated by the 3σ rule.

Moreover, the developed fluorimetric method was applied for practically probing Cys with various levels spiked in the samples of hela cells extractions (Fig. 8A). Accordingly, Cys in cell extractions could be detected over the linear concentration range from 0.0032 to 32.0 μM (R^2 = 0.9849), with the limit of detection of about 2.0 nM, which should be practically feasible for exploring Cys in hela cells with the concentrations of μM levels [43]. In addition, the fluorimetric test strips were employed to evaluate Cys with different concentrations spiked in human serum, showing the linear concentrations ranging from 0.0020 to 100.0 μM (R^2 = 0.9758), with the LOD of about 1.0 nM (Fig. 8B). Therefore, the fluorimetric strategy of test strips can promise the feasible applications for detecting Cys in cells and serum samples.

4. Conclusions

In summary, a solid-state fluorimetric strategy with test strips has been initially developed using Au-Ag nanospheres and ZIF-8 MOFs for the detection of Cys in hela cells and serum samples. Herein, Au-Ag nanospheres were prepared by the protein-templated biominerization route and harvested by the ethanol-aided desolvation route. As expected, the resulting nanospheres could present strong FL intensities that could be specifically quenched by Cys, presumably due to the Cys-mediated electrostatic interaction for cross-linking nanospheres and Cys-etched Ag atoms on Au-Ag nano-probes surfaces. Furthermore, the fluorimetric Cys test strips were fabricated by being coated first with the Au-Ag nanospheres and then ZIF-8 shells by using a vacuum-aided fast drying route with super-hydrophobic patterns, which could suppress the “Coffee stains” toward the uniform coatings of nano-probes on strips. Moreover, it was discovered that the introduction of ZIF-8 coatings could endow the test strips with dramatically improved environmental and storage stabilities over time in addition to the further enhanced FL intensities. The developed fluorimetric test strips were subsequently applied for the direct evaluation of Cys levels in hela cells extractions (down to about 2.0 nM) and serum with high analysis selectivity, sensitivity, and reproducibility, thus promising the potential applications for rapid and field-employable monitoring of Cys in the clinical laboratory. More importantly, this proposed fabrication protocol for stable and uniform fluorimetric test strips using MOFs coatings and super-hydrophobic patterns may pave the way towards the extensive applications for constructing a variety of solid-statetesting platforms in the biomedical, environmental, and food analysis fields.

Acknowledgments

This work is supported by the National Natural Science Foundations of China (No. 21675099), Major Basic Research Program of Natural Science Foundation of Shandong Province (ZR2018ZC0129), and Key R

&D Plan of Jining City (2018HMNS001), Shandong, P. R. China.

References

[1] E. Weerapana, C. Wang, G.M. Simon, F. Richter, S. Khare, M.B. Dillon, Quantitative reactivity profiling predicts functional cysteines in proteomes, Nature 468 (2010) 790–795.

[2] K.G. Reddie, K.S. Carroll, Expanding the functional diversity of proteins through cysteine oxidation, Curr. Opin. Chem. Biol. 12 (2008) 746–754.

[3] L. Li, B. Li, Sensitive and selective detection of cysteine using gold nanoparticles as colorimetric probes, Analyst 134 (2009) 1361–1365.

[4] S.K. Sun, K.X. Tu, X.P. Yan, The in vivo sparing of methionine by cysteine in sulfur amino acidrequirements in animal models and adult humans, Analyst 137 (2012) 2124–2128.

[5] W. Zhang, Z. Shi, F. Zhang, X. Liu, J. Jin, L. Jiang, Lead phthalocyanine as a selective carrier for preparation of a cysteine-selective electrode, Am. Cancer Soc. 25 (2013) 2071–2076.

[6] J. Liang, Z. Chen, L. Guo, L. Li, Chronically and acutely exercised rats biomarkers of oxidative stress and endogenous antioxidants, Chem. Commun. 47 (2011) 5476–5478.

[7] J.M. Zen, A.S. Kumar, J.C. Chen, Case-control study of plasma folate, homocysteine, vitamin B12, and cysteine as markers of cervical dysplasia, Anal. Chem. 73 (2001) 1169–1175.

[8] S. Shahrokhian, Lead phthalocyanine as a selective carrier for preparation of a cysteine-selective electrode, Anal. Chem. 73 (2001) 5972–5978.

[9] S. Huang, A simple and sensitive method for l-cysteine detection based on the fluorescence intensity increment of quantum dots, Anal. Chim. Acta 645 (2009) 73–78.

[10] Y.D. Zhao, W.D. Zhang, H. Chen, Q.M. Luo, Electrocatalytic oxidation of cysteine at carbon nanotube powder microelectrode and its detection, Sens. Actuators B 92 (2003) 279–285.

[11] G. Hignett, S. Threlfell, A.J. Wain, N.S. Lawrence, S.J. Wilkins, J. Davis, Electroanalytical exploitation of quinone-thiol interactions: application to the selective determination of cysteine, Analyst 126 (2001) 353–357.

[12] Y.V. Tcherkas, A.D. Denisenko, Simultaneous determination of several amino acids, including homocysteine, cysteine and glutamic acid, in human plasma by isocratic reversed-phase high-performance liquid chromatography with fluorimetric detection, J. Chromatogr. A 913 (2001) 309–313.

[13] C.M. Pfeiffer, D.L. Huff, E.W. Gunter, Rapid and accurate HPLC assay for plasma total homocysteine and cysteine in a clinical laboratory setting, Clin. Chemistry 45 (1999) 290–292.

[14] S. Wang, X. Feng, J. Yao, L. Jiang, Controlling wettability and photochromism in a dual-responsive tungsten oxide film, Angew. Chem. 45 (2006) 1264–1267.

[15] W. Jin, Y. Wang, Determination of cysteine by capillary zone electrophoresis with end-column amperometric detection at a gold/mercury amalgam microelectrode without deoxygenation, J. Chromatogr. A 769 (1997) 307–314.

[16] G. Chwatko, E. Bald, Determination of cysteine in human plasma by high-performance liquid chromatography and ultraviolet detection after pre-column derivatization with 2-chloro-1-methylpyridinium iodide, Talanta 52 (2000) 509–515.

[17] F. Andersen, J.F. Lynch, V.M. Anslyn, E.V. Anslyn, Naked-eye detection of histidine by regulation of Cu(II) coordination modes, Chemistry 11 (2005) 5319–5326.

[18] A. Zinellu, S. Sotgia, E. Pisanu, B. Scanu, Sanna, M. Deiana, L. Carru, Quantification of histidine, 1-methylhistidine and 3-methylhistidine in plasma and urine by capillary electrophoresis UV-detection, J. Sep. Sci. 33 (2010) 3781–3785.

[19] X. Yuan, Y. Tay, X. Dou, Z. Luo, D.T. Leong, J. Xie, Glutathione-protected silver nanoclusters as cysteine-selective fluorometric and colorimetric probe, Anal. Chem. 85 (2013) 1913–1919.

[20] M. Liu, N. Li, Y. He, Y. Ge, G. Song, Dually emitting gold-silver nanoclusters as viable ratiometric fluorescent probes for cysteine and arginine, Mikrochim. Acta 185 (2018) 147–155.

[21] Y. Cai, L. Feng, Y. Hua, H. Liu, M. Yin, H. Wang, Q-Graphene-loaded metal organic framework nanocomposites with water-triggered fluorescence turn-on: fluorimetric test strips for directly sensing trace water in organic solvents, Chem. Commun. 54 (2018) 13595–13598.

[22] Y. Qiao, J. Shang, S. Li, L. Feng, H. Wang, Fluorimetric mercury test strips with suppressed "coffee stains" by a bio-inspired fabrication strategy, Sci. Rep. 6 (2016) 36494–36502.

[23] Z. Duan, M. Yin, C. Zhang, G. Song, H. Wang, Polyhydric polymer-loaded pyrene composites as powerful adsorbents and fluorescent probes: highly efficient adsorption and test strips-based fluorimetric analysis of curcumin in urine and plant extracts, Analyst 143 (2018) 392–395.

[24] S. Lv, Y. Tang, K. Zhang, D. Tang, Wet NH_3-triggered NH_2-MIL-125(Ti) structural switch for visible fluorescence immunoassay impregnated on paper, Anal. Chem. 90 (2018) 14121–14125.

[25] K. Liang, R. Ricco, C.M. Doherty, M.J. Styles, S. Bell, N. Kirby, Biomimetic mineralization of metal-organic frameworks as protective coatings for biomacromolecules, Nat. Commun. 6 (2015) 7240–7248.

[26] S. Choi, R.M. Dickson, J. Yu, Developing luminescent silver nanodots for biological applications, Chem. Soc. Rev. 41 (2012) 1867–1891.

[27] H. Jans, Q. Huo, Gold nanoparticle-enabled biological and chemical detection and analysis, Chem. Soc. Rev. 41 (2012) 2849–2866.

[28] K. Saha, S.S. Agasti, C. Kim, X. Li, V.M. Rotello, Gold nanoparticles in chemical and biological sensing, Chem. Rev. 112 (2012) 2739–2779.

[29] Y. Lu, W. Chen, Sub-nanometre sized metal clusters: from synthetic challenges to the unique property discoveries, Chem. Soc. Rev. 41 (2012) 3594–3623.

[30] C. Fan, X. Lv, F. Liu, L. Feng, M. Liu, Y. Cai, H. Wang, Silver nanoclusters encapsulated into metal-organic frameworks with enhanced fluorescence and specific ion accumulation toward the microdot array-based fluorimetric analysis of copper in blood, ACS Sens. 3 (2018) 441–450.

[31] L. Feng, M. Liu, H. Liu, C. Fan, Y. Cai, L. Chen, H. Wang, High-throughput and sensitive fluorimetric strategy for microRNAs in blood using wettable microwells array and silver nanoclusters with red fluorescence enhanced by metal organic frameworks, ACS Appl. Mater. Interfaces 10 (2018) 23647–23656.

[32] S. Xu, T. Gao, X. Feng, X. Fan, G. Liu, Y. Mao, Near infrared fluorescent dual ligand functionalized Au NCs based multidimensional sensor array for pattern recognition of multiple proteins and serum discrimination, Biosens. Bioelectron. 97 (2017) 203–207.

[33] N. Zhang, Y. Si, Z. Sun, L. Chen, R. Li, Y. Qiao, H. Wang, Rapid, selective, and ultrasensitive fluorimetric analysis of mercury and copper levels in blood using bimetallic gold-silver nanoclusters with “silver effect”-enhanced red fluorescence, Anal. Chem. 86 (2014) 11714–11721.

[34] W. Zhang, Y. Tang, D. Du, J. Smith, C. Timchalk, D. Liu, Direct analysis of trichloropyridinol in human saliva using an Au nanoparticles-based immunochromatographic test strip for biomonitoring of exposure to chlorpyrifos, Talanta 114 (2013) 261–267.

[35] R. Sadeghi, A.A. Moosavi-Movahedi, Z. Emam-jomeh, A. Kalbasi, S.H. Razavi, M. Karimi, The effect of different desolvating agents on BSA nanoparticle properties and encapsulation of curcumin, J. Nanopart. Res. 16 (2014) 2565–2579.

[36] D. Wang, R. Cai, S. Sharma, J. Jirak, S.K. Thummanapelli, N.G. Akhmedov, Silver effect" in gold(I) catalysis: an overlooked important factor, J. Am. Chem. Soc. 134 (2012) 9012–9019.

[37] J. Xie, Y. Zheng, J.Y. Ying, Highly selective and ultrasensitive detection of Hg(2+) based on fluorescence quenching of Au nanoclusters by Hg(2+)-Au(+) interactions, Chem. Commun. 46 (2010) 961–963.

[38] Y. Lv, M. Lu, Y. Yang, Y. Yin, J. Zhao, Electrochemical detection of intracellular glutathione based on ligand exchange assisted release of DNA-templated silver nanoparticles, Sens. Actuators B Chem. 244 (2017) 151–156.

[39] S. Li, Z. Sun, R. Li, M. Dong, L. Zhang, W. Qi, H. Wang, ZnO nanocomposites modified by hydrophobic and hydrophilic silanes with dramatically enhanced tunable fluorescence and aqueous ultrastability toward biological imaging applications, Sci. Rep. 5 (2015) 8475–8482.

[40] R.W. Huang, Y.S. Wei, X.Y. Dong, X.H. Wu, C.X. Du, S.Q. Zang, Hypersensitive dual-function luminescence switching of a silver-chalcogenolate cluster-based metal-organic framework, Nat. Chem. 9 (2017) 689–697.

[41] P.K. Sudeep, S.T.S. Joseph, T.K. George, Selective detection of cysteine and glutathione using gold nanorods, J. Am. Chem. Soc. 127 (2005) 6516–6517.

[42] A.E. Brodi, J. Potter, D.J. Reed, Unique characteristics of rat spleen lymphocyte, L1210 lymphoma and Hela cellsin glutathione biosynthesis from sulfur-containing amino acids, Eur. J. Biochem. 123 (1982) 159–164.

[43] B.Y. Han, J.P. Yuan, E.K. Wang, Sensitive and selective sensor for biothiols in the cell based on the recovered fluorescence of the CdTe quantum dots-Hg (II) system, Anal. Chem. 8113 (2009) 5569–5573.

Yuanyuan Cai received her bachelor degree in Chemistry Education from the Qufu Normal University in China, in 2016, and now is a postgraduate student in Analytical Chemistry at the same university. Her research interests include Biosensors and Medical Detectors R&D.

Yue Hua received her bachelor degree in Chemistry Education from the Jining University in China, and now is a postgraduate student in Analytical Chemistry at the Qufu Normal University. Her research interests include Biosensors and Medical Detectors R&D.

Mengyuan Yin received her bachelor degree in Chemical Engineering and Technology from the Qufu Normal University in Chin and now is a postgraduate student in Analytical Chemistry at the same university. Her research interests include Biosensors and Medical Detectors R&D.

Huan Liu received her bachelor degree in Chemical Engineering and Technology from the Qufu Normal University in China, and now is a postgraduate student in Analytical Chemistry at the same university. Her research interests include Biosensors and Medical Detectors R&D.

Shuai Li received his Ph.D in Analytical Chemistry from the East China Normal University in China. His research interests include Biosensors and Medical Detectors R&D.

Fengxiang Wang received his Ph.D from Nanjing University of Science and Technology, China, in 2016, and now is working at Qufu Normal University as an associate professor in Chemistry. His research interests mainly include Biosensors and Medical Detectors R&D.

Hua Wang received his Ph.D from Hunan University, China, in 2004, and now is working at Qufu Normal University as a distinguished professor in Chemistry. His research interests mainly include Chemo/Biosensors, Advanced Functional Materials, and Organic Synthesis.